Submitted to ApJL

A Smoking Gun in the Carina Nebula

Kenji Hamaguchi[1,2], Michael F. Corcoran[1,3], Yuichiro Ezoe[4], Leisa Townsley[5], Patrick Broos[5], Robert Gruendl[6], Kaushar Vaidya[6,a], Stephen M. White[7], Rob Petre[8], You-Hua Chu[6]

ABSTRACT

The Carina Nebula is one of the youngest, most active sites of massive star formation in our Galaxy. In this nebula, we have discovered a bright X-ray source that has persisted for ~30 years. The soft X-ray spectrum, consistent with kT ~130 eV blackbody radiation with mild extinction, and no counterpart in the near- and mid-infrared wavelengths indicate that it is a $\sim 10^6$-year-old neutron star housed in the Carina Nebula. Current star formation theory does not suggest that the progenitor of the neutron star and massive stars in the Carina Nebula, in particular η Car, are coeval. This result demonstrates that the Carina Nebula experienced at least two major episodes of massive star formation. The neutron star would be responsible for remnants of high energy activity seen in multiple wavelengths.

Subject headings: supernova remnants — stars: evolution — stars: formation — stars: neutron — ISM: bubbles — X-rays: stars

1. Introduction

Massive stars ($M \gtrsim 10 M_\odot$) are born from giant molecular clouds along with many lower mass stars, forming a stellar cluster or association. Massive stars evolve orders of magnitude more quickly

[1]CRESST and X-ray Astrophysics Laboratory NASA/GSFC, Greenbelt, MD 20771

[2]Department of Physics, University of Maryland, Baltimore County, 1000 Hilltop Circle, Baltimore, MD 21250

[3]Universities Space Research Association, 10211 Wincopin Circle, Suite 500, Columbia, MD 21044

[4]Tokyo Metropolitan University, 1-1, Minami-Osawa, Hachioji, Tokyo, 192-0397, Japan

[5]Department of Astronomy and Astrophysics, Pennsylvania State University, 525 Davey Laboratory, University Park, PA 16802

[6]Department of Astronomy, University of Illinois, Urbana, IL 61801

[7]Department of Astronomy, University of Maryland, College Park, MD 20742

[8]Astrophysics Science Division, NASA Goddard Space Flight Center, Greenbelt, MD 20771

[a]previously Kaushar Sanchawala

than lower mass stars, and die through supernovae or hypernovae explosions in $\lesssim 10^7$ years. High interstellar pressures that massive stars produce through their strong UV radiation and supernova explosions can compress a pre-existing cloud and trigger the formation of new stars (cf. Elmegreen 1998).

The Carina Nebula is one of the most massive star forming regions in our Galaxy. It contains two massive stellar clusters, Trumpler 14 and 16 (Figure 1), possessing over 50 massive stars with spectral types earlier than O6 ($\gtrsim 40\ M_\odot$, Smith 2006). The nebula is also home to one of the most massive stars in our Galaxy, η Carinae, which has an estimated initial mass $\gtrsim 150\ M_\odot$ and a current mass of about 90 $M_\odot$ (Hillier et al. 2001).

At a distance of only $\sim$2.3 kpc (Davidson & Humphreys 1997), the Carina Nebula is one of the best sites for studying how very massive stars form and affect their environment. It shows signatures of violent activities: a bipolar supershell structure (Smith et al. 2000), strong turbulence in interstellar clouds (Yonekura et al. 2005), and hot X-ray plasma through the entire nebula (Seward et al. 1979; Townsley 2006; Hamaguchi et al. 2007; Ezoe et al. 2008). Two primary mechanisms have been proposed to produce these structures. One is strong winds and UV radiation from massive stars in the nebula, while the other is supernova explosions. The energy budget and elemental abundance distribution favor the supernova mechanism (Yonekura et al. 2005; Hamaguchi et al. 2007). However, neither black hole, neutron star, nor clear remnant from a supernova, has been found in the Carina Nebula. In addition, any massive supernova progenitor is unlikely to be co-eval with the observed stars since it would have had to be more massive than η Car; this means that, if a supernova occurred in the Carina Nebula, its progenitor would probably have had to have formed much earlier than η Car. Thus, detection of any compact object in the Carina Nebula would be of vital interest for understanding the star formation history of the region.

From multiple sets of X-ray data, we found a promising neutron star candidate at the heart of the Carina Nebula. The source, which we call EHG7 (Ezoe et al. 2008), was detected as a very soft source in X-ray images 8.5′ southeast of η Car, equivalent to 5.7 pc in the projected physical distance assuming d =2.3 kpc (See Figure 1). The X-ray source has also been reported contemporaneously in three other papers (Albacete Colombo et al. 2003; Ezoe et al. 2008; Pires & Motch 2008), one of which also suggested EHG7 as a neutron star based on *XMM-Newton* data (Pires & Motch 2008). However, these analyses lacked the spatial resolution to accurately determine the source position in order to look for possible counterparts at other wavelengths, nor were the source properties investigated in any detail. This paper presents a comprehensive study of the characteristics of EHG7 using all available X-ray data to present conclusive evidence of the compact nature of EHG7.

2. Observations

We searched the HEASARC archive for data sets with EHG7 in the fields of view and found 28 X-ray observations with spatial resolution better than 1′. These observations are listed in Table 1. Observations with lower spatial resolution telescopes and/or instruments (e.g. *Einstein* IPC, *ASCA*) failed to detect EHG7 due to severe contamination from surrounding soft diffuse X-ray emission. Throughout this document, individual *Einstein*, *ROSAT*, *XMM-Newton*, and *Chandra* observations are designated EIN, ROS, XMM, CXO respectively, subscripted with the year, month, and day of the start time of the observations.

We used SAS version 7.0.0 for analysis of the *XMM-Newton* data and CIAO version 4.0 for analysis of the *Chandra* spectral and timing data. For source position determination on the *Chandra* image, we used a custom analysis method for *Chandra* data sets developed by the Pennsylvania State University (see details in Broos et al. 2007, Broos et al. in prep.). We analyzed all other data sets and performed generic light curve and spectral analysis using HEAsoft version 6.5.1. We utilized the pipeline products of each data set for data screening, such as excluding high background intervals and noise events.

3. Results

The *Chandra* observation CXO_{080905}, performed as a part of a Very Large Project to map the Carina Nebula in X-rays (PI: Leisa Townsley), gives the most precise and reliable absolute position of EHG7 (Figure 2). In this observation, EHG7 was imaged 6.7′ off-axis on the ACIS-I detector. The absolute coordinates of the source were determined to be (*R.A.*, *Decl.*)[*J2000*] = ($10^{h}46^{m}08.72^{s}$, $-59°43'06.5''$) with less than 1″ positional uncertainty after correcting the Chandra astrometry with cross correlation of other X-ray sources with infrared sources in the 2MASS catalogue and correlating the PSF at the location of this source with the image of the source.

We searched for near- and mid-infrared counterparts from images obtained with the IRSF (InfraRed Survey Facility) 1.4m telescopes (see Sanchawala et al. 2007a,b, for details) and in all available *Spitzer* InfraRed Array Camera (IRAC; Fazio et al. 2004) observations combined, but these images showed no counterpart object within the error circle of the X-ray source (Figure 2). We used standard aperture photometry routines in IRAF to estimate the 3-σ upper-limits, which were 18.5 mag, 19.5 mag and 18.5 mag in the J, H and K_S bands and 0.84, 0.51, 4.7, and 13.6 mJy in the IRAC 3.6, 4.5, 5.8, and 8.0 μm bands, respectively. Assuming blackbody spectra with temperatures between 2000 and 10000 K, the bolometric flux of EHG7 was limited to $<5\times10^{-13}$ ergs cm^{-2} s^{-1}.

X-ray emission from EHG7 was detected at above 3σ significance in all observations in Table 1 except for 5 *ROSAT* observations with short exposures. None of these observations showed any significant time variation from EHG7 at greater than 90% confidence in a fit of each light curve in the whole instrumental energy band with a constant flux model. For data sets with no spectral

resolution and/or poor photon statistics, we measured the photon count rate or upper limit in whole band images using the `sosta` package in `ximage`, taking a suitable nearby source free region as background. We then converted the source counts to energy flux using the `PIMMS` tool, assuming blackbody radiation with $kT \sim$126 eV and $N_{\rm H} \sim 3.4\times10^{21}$ cm^{-2}, derived from a best-fit model to the *XMM-Newton* spectrum as described below. For the other data sets, we measured source flux from time averaged spectra, assuming the same spectral model. The results are shown in Table 1. EHG7 did not show any significant flux variation above ∼20% between the observations. A formal fit of these data rejected a constant flux model at above 90% confidence, but this result is probably due to calibration uncertainties between different instruments or pointings. The X-ray emission was stable for ∼30 years with $F_{\rm X}$ (0.3–2 keV) $\sim 9.6\times10^{-13}$ ergs cm^{-2} s^{-1}.

Individual observations did not have sufficient photon statistics for detailed spectral analysis. Since the spectral shape did not change significantly between observations, we combined all the source spectra taken between 2000 and 2006 with the *XMM-Newton* MOS detectors (Figure 3). The combined X-ray spectrum showed significant emission only below 2 keV and is almost featureless except for a slight dip at around 0.9 keV and a strong dip at around 0.6 keV, which is perhaps produced by oxygen edge absorption in the interstellar medium. The spectrum can be reproduced using a 1-temperature optically-thin thermal plasma emission model suffering absorption by neutral gas along the line of sight (Table 2), but the best-fit model has an unusually small elemental abundance of $\lesssim 10^{-3}$ solar, without evidence of emission lines from oxygen, iron, or neon atoms near 0.5–1 keV. The spectrum also can be fit by a 1-temperature blackbody emission model with a temperature of 0.13±0.01 keV (90% confidence) suffering absorption by neutral gas with hydrogen column density of $3.4\pm0.6\times10^{21}$ cm^{-2} (90% confidence). The spectrum could not be adequately fit using an absorbed power law model.

The ratio of the X-ray flux to the bolometric flux, $\log F_{\rm X}/F_{\rm bol} > -0.7$, was significantly larger than that typically seen in stellar X-ray emission ($\lesssim -3$, Gagné et al. 1995). This large $F_{\rm X}/F_{\rm bol}$ means that EHG7 is unlikely to be a star in the Carina star-forming complex nor in the fore- and background but must be a compact object such as a black hole or a neutron star. The X-ray characteristics of this source, a single temperature blackbody spectrum without time variation longer than hourly timescales, are typical of isolated neutron stars, where the emission comes from the cooling neutron star surface. It is unlikely to be a black hole, which would show strong time variation on both short and long timescales, reflecting activity around the accretion disk near the event horizon. All this evidence shows that the source is most likely a neutron star.

The hydrogen column density is consistent with interstellar absorption to the Carina Nebula ($\sim 3\times10^{21}$ cm^{-2}, see discussion in Leutenegger et al. 2003). The 90% confidence upper limit (4.0×10^{21} cm^{-2}) is much smaller than absorption through our Galaxy ($\sim 1.2\times10^{22}$ cm^{-2}, Kalberla et al. 2005), which emission from an AGN should suffer. It is also significantly smaller than absorption to the background stars in the field, which have visual extinctions twice as large as Carina cluster members (DeGioia-Eastwood et al. 2001). This result suggests that EHG7 is in front of the molecular cloud that lies behind the Trumpler 14 and 16 clusters, and neighbors the Carina

Nebula.

We found no radio counterpart of EHG7 in a continuum radio map of the Carina region from the Southern Galactic Plane Survey (McClure-Griffiths et al. 2005), but the resolution of these data is only $1'$ and weak point sources will not be detected against the strong nebular radio sources Car I and Car II. The ATNF Pulsar Catalogue (Manchester et al. 2005) lists 11 pulsars within 2° of EHG7, but no source coincident with EHG7 itself. We detected no significant pulses from EHG7 in the X-ray data using a fast Fourier transform, including the EPIC/PN data in XMM_{060131} and XMM_{041207} which had relatively fine timing resolution (73.35 msec). However, many neutron stars do not pulse in X-rays, and young neutron stars generally show fast pulse periods of less than several hundred milli-second (e.g. De Luca et al. 2005) which would be too fast to be detectable in the XMM data.

4. Discussion

The intrinsic X-ray luminosity is 4.8×10^{32} ergs s^{-1} or equivalent to an emitting radius of $\sim$7.2 km (d =2.3 kpc). Assuming the standard cooling curve of a M =1.4 $M_\odot$ neutron star (Tsuruta 2006), the age of EHG7 is estimated at $\sim0.5-1\times10^6$-year. The blackbody temperature, 0.13 keV, is also typical of neutron stars older than 1000 years (e.g. 1E1207.4-5209, PSR B0656+14 and PSR B1055-52, Sanwal et al. 2002; De Luca et al. 2005). If the dip feature in the XMM spectrum at $\sim$0.9 keV is produced by fundamental cyclotron absorption, the magnetic field strength is $\sim7.5\times10^{10}$ Gauss, at the lower boundary of the magnetic field strength of young radio pulsars in the 10^{3-7} year age range (e.g. Reisenegger 2001). The X-ray spectrum did not show a non-thermal power-law component in the hard band that would typically originate from charged particles in the magnetosphere. The upper limit of L_X [0.5–10 keV] $< 6.4\times10^{30}$ ergs s^{-1} estimated from a fit of the spectrum above 2 keV assuming an additional power-law component with a fixed Γ =1.7 is similarly lower than other middle-aged rotation-powered pulsars of a few $\times10^5$ year old (De Luca et al. 2005; Manzali et al. 2007). These results suggest that the neutron star originated in a supernova explosion about 10^6 years ago. Although no X-ray observation detected a pulsation from the source, not all neutron stars are observed pulsars; in particular, middle-aged neutron stars have short pulsation periods (less than a few hundred milli-second), and the existing X-ray data did not have enough time resolution to detect such a short pulse.

Two other neutron stars have been discovered near other star forming regions (Figer et al. 2005; Muno et al. 2006). Both of them have characteristics of magnetars — neutron stars with strong magnetic fields up to 10^{15} Gauss — which exploded within the last $\sim10^4$ years and whose progenitors might represent the high mass end of stars born in these star forming regions. However, the neutron star discovered in the Carina Nebula cannot be co-eval with the current generation of stars. Since the higher mass stars evolve faster, the progenitor of the neutron star would have to be more massive than η Car. Eta Car's estimated initial mass $\gtrsim$150 $M_\odot$ (Hillier et al. 2001) is much higher than the conventional progenitor mass of neutron stars (less than $\sim$25 $M_\odot$) and explosion of

such a massive star would likely produce a black hole, instead of a neutron star (although Woosley et al. 2002, found that explosions of stars with masses up to $\sim$60 $M_{\odot}$ may produce a neutron star under certain circumstances).

Based on standard stellar evolution models, the progenitor of the neutron star should have been born $6-30\times10^6$ year ago with an initial mass between $8-25$ $M_{\odot}$. This is significantly earlier than formation of the massive stars in the Trumpler 14 and 16 clusters which occurred less than 3×10^6 years ago (DeGioia-Eastwood et al. 2001; Massey et al. 2001). This suggests that the Carina Nebula has experienced at least 2 episodes of star formation. This is consistent with stellar population studies (DeGioia-Eastwood et al. 2001) which also suggest that intermediate-mass stars have formed continuously over the last 10^7 years.

The last episode of star formation in the Carina Nebula appears to have been nearly contemporaneous with the supernova explosion of the progenitor of this neutron star. This may suggest that the expanding H II region, wind-brown bubble and/or supernova explosion of this star (and perhaps others yet undetected) played a role in triggering the last episode of star formation. Although the neutron star is currently well away from the nebula center, it could have moved the projected distance in $\sim10^6$ year with a transverse velocity of $\sim$6 km s^{-1}, which is well within the range of typical kick velocities of radio pulsars (several hundred km s^{-1}, Lyne & Lorimer 1994).

Discovery of a neutron star supports the argument that the diffuse high energy emission observed in the Carina Nebula originated in an ancient supernova explosion. Some measurements require multiple supernova explosions in this field (Yonekura et al. 2005; Hamaguchi et al. 2007), so that the neutron star may be one of multiple neutron stars and black holes hidden in the Carina Nebula. If the soft extended X-ray plasma in reality heated up by supernova explosions $\sim10^6$ years ago, it would represent an important phase of the evolution of inter stellar medium when hot gas produced by supernova remnants merges together to form the "hot ionized intercloud medium (HIM)" component (McKee & Ostriker 1977). The result may have implications for the origin of diffuse X-ray emission observed now from many star forming regions (Townsley et al. 2003; Güdel et al. 2008).

The Carina Nebula is a nearby star forming complex containing some of the most massive stars yet identified. With its relatively small interstellar extinction the Carina Nebula is one of the best regions to search for weak signals from neutron stars and inactive black holes, the relics of earlier epochs of massive star formation, and to study the formation mechanism of very massive stars. These kinds of sources efficiently emit high energy X-rays and γ-ray photons, so observations at these wavelengths, in particular the Fermi Gamma-ray Observatory, will be useful to survey such sources embedded in star formation regions.

We are grateful to T.R. Gull and K.E. Nielsen for useful comments. This work is performed while K.H. was supported by the NASA Astrobiology Program under CAN 03-OSS-02. This research has made use of data obtained from the High Energy Astrophysics Science Archive Research

Center (HEASARC), provided by NASA's Goddard Space Flight Center.

Facilities: CXO (ACIS-I), XMM-Newton (EPIC), ROSAT (PSPC, HRI), EINSTEIN (HRI) Spitzer (IRAC), IRSF

REFERENCES

Albacete Colombo, J. F., Méndez, M., & Morrell, N. I. 2003, MNRAS, 346, 704

Broos, P. S., Feigelson, E. D., Townsley, L. K., Getman, K. V., Wang, J., Garmire, G. P., Jiang, Z., & Tsuboi, Y. 2007, ApJS, 169, 353

Davidson, K., & Humphreys, R. M. 1997, ARA&A, 35, 1

De Luca, A., Caraveo, P. A., Mereghetti, S., Negroni, M., & Bignami, G. F. 2005, ApJ, 623, 1051

DeGioia-Eastwood, K., Throop, H., Walker, G., & Cudworth, K. M. 2001, ApJ, 549, 578

Elmegreen, B. G. 1998, in Astronomical Society of the Pacific Conference Series, Vol. 148, Origins, ed. C. E. Woodward, J. M. Shull, & H. A. Thronson, Jr., 150

Ezoe, Y., Hamaguchi, K., Gruendl, R. A., Chu, Y.-H., Petre, R., & Corcoran, M. F. 2008, PASJ, in print (astro-ph/0809.3495)

Fazio, G. G., and 64 others, 2004, ApJS, 154, 10

Figer, D. F., Najarro, F., Geballe, T. R., Blum, R. D., & Kudritzki, R. P. 2005, ApJ, 622, L49

Gagné, M., Caillault, J. P., & Stauffer, J. R. 1995, ApJ, 445, 280

Güdel, M., Briggs, K. R., Montmerle, T., Audard, M., Rebull, L., & Skinner, S. L. 2008, Science, 319, 309

Hamaguchi, K., and 11 others, 2007, PASJ, 59, 151

Hillier, D. J., Davidson, K., Ishibashi, K., & Gull, T. 2001, ApJ, 553, 837

Kalberla, P. M. W., Burton, W. B., Hartmann, D., Arnal, E. M., Bajaja, E., Morras, R., & Pöppel, W. G. L. 2005, A&A, 440, 775

Leutenegger, M. A., Kahn, S. M., & Ramsay, G. 2003, ApJ, 585, 1015

Lyne, A. G., & Lorimer, D. R. 1994, Nature, 369, 127

Manchester, R. N., Hobbs, G. B., Teoh, A., & Hobbs, M. 2005, AJ, 129, 1993

Manzali, A., De Luca, A., & Caraveo, P. A. 2007, ApJ, 669, 570

Massey, P., DeGioia-Eastwood, K., & Waterhouse, E. 2001, AJ, 121, 1050

McClure-Griffiths, N. M., Dickey, J. M., Gaensler, B. M., Green, A. J., Haverkorn, M., & Strasser, S. 2005, ApJS, 158, 178

McKee, C. F., & Ostriker, J. P. 1977, ApJ, 218, 148

Muno, M. P., and 11 others, 2006, ApJ, 636, L41

Pires, A. M., & Motch, C. 2008, in American Institute of Physics Conference Series, Vol. 983, 40 Years of Pulsars: Millisecond Pulsars, Magnetars and More, ed. C. Bassa, Z. Wang, A. Cumming, & V. M. Kaspi, 363–365

Reisenegger, A. 2001, in Astronomical Society of the Pacific Conference Series, Vol. 248, Magnetic Fields Across the Hertzsprung-Russell Diagram, ed. G. Mathys, S. K. Solanki, & D. T. Wickramasinghe, 469

Sanchawala, K., Chen, W.-P., Lee, H.-T., Chu, Y.-H., Nakajima, Y., Tamura, M., Baba, D., & Sato, S. 2007a, ApJ, 656, 462

Sanchawala, K., and 8 others, 2007b, ApJ, 667, 963

Sanwal, D., Pavlov, G. G., Zavlin, V. E., & Teter, M. A. 2002, ApJ, 574, L61

Seward, F. D., Forman, W. R., Giacconi, R., Griffiths, R. E., Harnden, F. R. J., Jones, C., & Pye, J. P. 1979, ApJ, 234, L55

Smith, N. 2006, MNRAS, 367, 763

Smith, N., Egan, M. P., Carey, S., Price, S. D., Morse, J. A., & Price, P. A. 2000, ApJ, 532, L145

Townsley, L. K. 2006, in the STScI May Symposium, "Massive Stars: From Pop III and GRBs to the Milky Way, ed. M. Livio, (astro–ph/0608173)

Townsley, L. K., Feigelson, E. D., Montmerle, T., Broos, P. S., Chu, Y.-H., & Garmire, G. P. 2003, ApJ, 593, 874

Tsuruta, S. 2006, in American Institute of Physics Conference Series, Vol. 847, Origin of Matter and Evolution of Galaxies, ed. S. Kubono, W. Aoki, T. Kajino, T. Motobayashi, & K. Nomoto, 163–170

Woosley, S. E., Heger, A., & Weaver, T. A. 2002, Reviews of Modern Physics, 74, 1015

Yonekura, Y., Asayama, S., Kimura, K., Ogawa, H., Kanai, Y., Yamaguchi, N., Barnes, P. J., & Fukui, Y. 2005, ApJ, 634, 476

Table 1. X-ray Observations with EHG7 in the Field of View

Abbreviation	Sequence ID	Observation Start	Detector/Filter	Exposure (ksec)	Flux (0.3–2 keV) (10^{-14} ergs cm^{-2} s^{-1})
EIN_{781214}	1074	1978 Dec. 14, 05:44	HRI-2	17.4	9.1±6.5
ROS_{900727}	RH150037N00	1990 Jul. 27, 00:12	HRI	3.3	<10.1
ROS_{911215}	RP200108N00	1991 Dec. 15, 9:58	PSPCB	1.6	<19.3
ROS_{920612}	RP900176N00	1992 Jun. 12, 22:33	PSPCB	23.6	9.3±1.3
ROS_{920731}	RH900385N00	1992 Jul. 31, 01:03	HRI	11.4	10.3±3.8
ROS_{920809}	RP201262N00	1992 Aug. 9, 22:21	PSPCB	5.7	14.1±5.4
ROS_{920810}	RP200709A01	1992 Aug. 10, 19:03	PSPCB	5.9	<21.6
ROS_{921215}	RP900176A01	1992 Dec. 15, 17:39	PSPCB	14.1	6.8±1.6
ROS_{940106}	RH900385A02	1994 Jan 6, 1:54	HRI	0.5	<69.2
ROS_{940721}	RH900385A03	1994 Jul. 21, 02:04	HRI	40.1	9.0±1.9
ROS_{960813}	RH900644N00	1996 Aug. 13, 21:07	HRI	1.7	<29.4
ROS_{971223}	RH202331N00	1997 Dec. 23, 08:59	HRI	46.5	8.1±1.7
XMM_{000726}	112580601	2000 Jul. 26, 05:08	MOS/thick	–/31.7/28.5	9.1±1.0
XMM_{000727}	112580701	2000 Jul. 27, 23:58	MOS/thick	–/10.3/7.5	9.0±1.9
XMM_{030125}	145740101	2003 Jan. 25, 12:58	MOS/thick	–/6.6/6.6	8.7±1.8
$XMM_{030127A}$	145740201	2003 Jan. 27, 01:04	MOS/thick	–/5.1/6.0	11.4±2.2
$XMM_{030127B}$	145740301	2003 Jan. 27, 20:37	MOS/thick	–/6.2/6.4	10.3±2.0
$XMM_{030129A}$	145740401	2003 Jan. 29, 01:41	MOS/thick	–/7.8/8.2	8.1±1.7
$XMM_{030129B}$	145740501	2003 Jan. 29, 23:55	MOS/thick	–/6.6/6.6	9.0±1.8
XMM_{030608}	160160101	2003 Jun. 08, 13:30	MOS/thick	–/12.5/13.0	10.6±1.7
XMM_{030613}	160160901	2003 Jun. 13, 23:52	MOS/thick	–/29.3/29.5	10.3±1.1
XMM_{030722}	145780101	2003 Jul. 22, 01:51	MOS/thick	–/8.0/8.1	8.8±2.0
XMM_{030802}	160560101	2003 Aug. 02, 21:01	MOS2/thick	–/–/9.7	11.4±2.6
XMM_{030809}	160560201	2003 Aug. 09, 01:44	MOS/thick	–/11.4/11.0	10.6±1.7
XMM_{030818}	160560301	2003 Aug. 18, 15:23	MOS/thick	–/17.4/17.5	9.9±1.2
XMM_{041207}	206010101	2004 Dec. 7, 7:30	PN/med	19.4/–/–	8.3±1.1
XMM_{060131}	311990101	2006 Jan. 31, 18:04	PN&MOS/thick	26.5/59.9/61.1	9.2±0.5
CXO_{080905}	900825	2008 Sep. 5, 21:24	ACIS-I	59.4	8.5±0.6

Note. — Abbreviation: abbreviation adopted for each observation. EIN: Einstein, ROS: ROSAT, XMM: XMM-Newton, CXO: Chandra, Sequence ID: sequence identification number of each observation. Detector/Filter: optical blocking filter for *XMM-Newton*, selected detectors for the others, Exposure: pn/MOS1/MOS2 for *XMM-Newton*, Flux: Error denotes the 90% confidence range. The upper limit is at a 3σ level.

Table 2. Spectral Fits

Model	kT (keV)	Abundance (solar)	$N_{\rm H}$ (10^{21}cm^{-2})	$L_{\rm X}$ (10^{32}ergs s^{-1})	$\Delta\chi^2$ (d.o.f)
1T APEC	0.17 (0.14–0.18)	$<6.6\times10^{-4}$	5.5 (5.2–6.4)	30	1.31 (67)
1T Blackbody	0.13 (0.12–0.13)	···	3.4 (2.8–4.0)	4.8	1.31 (68)

Note. — Absorption corrected $L_{\rm X}$ between 0.3–8 keV assuming d =2.3 kpc. The parentheses in the kT and $N_{\rm H}$ columns denote the 90% confidence range.

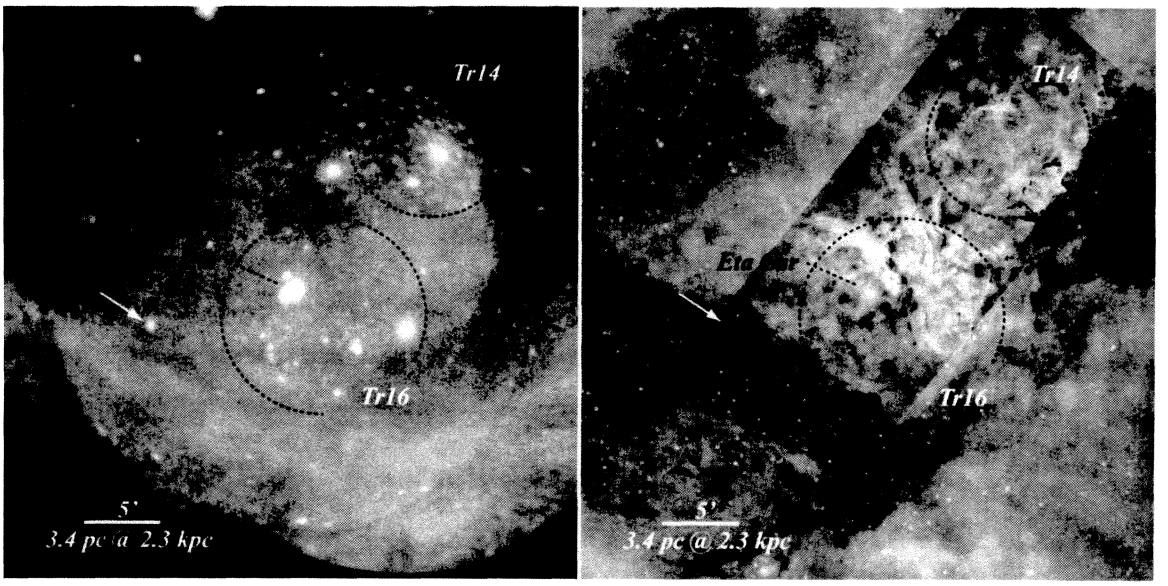

Fig. 1.— The central part of the Carina Nebula in X-rays (*Left*) and in optical wavelengths (*Right*). EHG7, the source discussed here, is denoted by the white arrow. It is located on the conspicuous V-shaped dark lane running across the optical image and is surrounded by diffuse X-ray emission. It is likely to be a neutron star in the Carina star-forming complex. The black dotted line and circles depict positions of the super massive star η Car and massive stellar clusters, Trumpler 14 and 16, respectively.

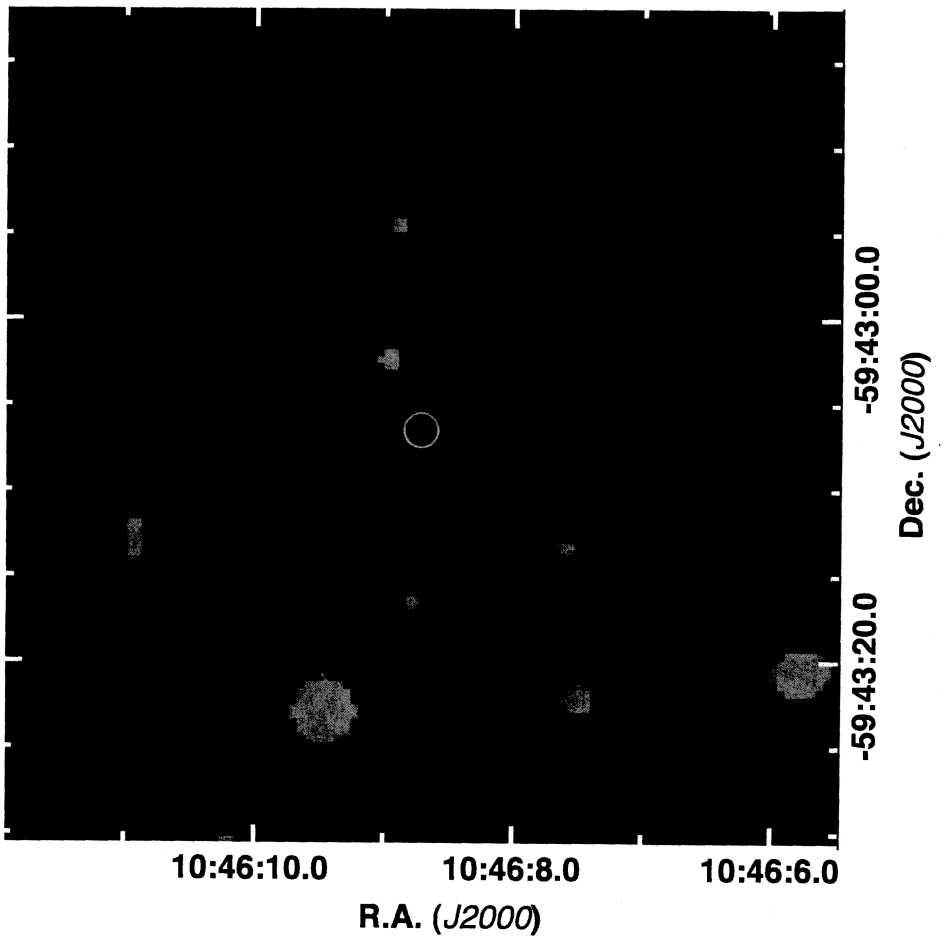

Fig. 2.— Magnified image of the neutron star field (*blue*: a *Chandra* X-ray image after the *PSF* image reconstruction, *red*: a deep H band image taken with the IRSF observatory). The position of the X-ray source EHG7 is marked with a green circle with a $1''$ radius; it has no infrared counterpart. Another X-ray source about $10''$ southwest from EHG7 has a counterpart in the H-band.

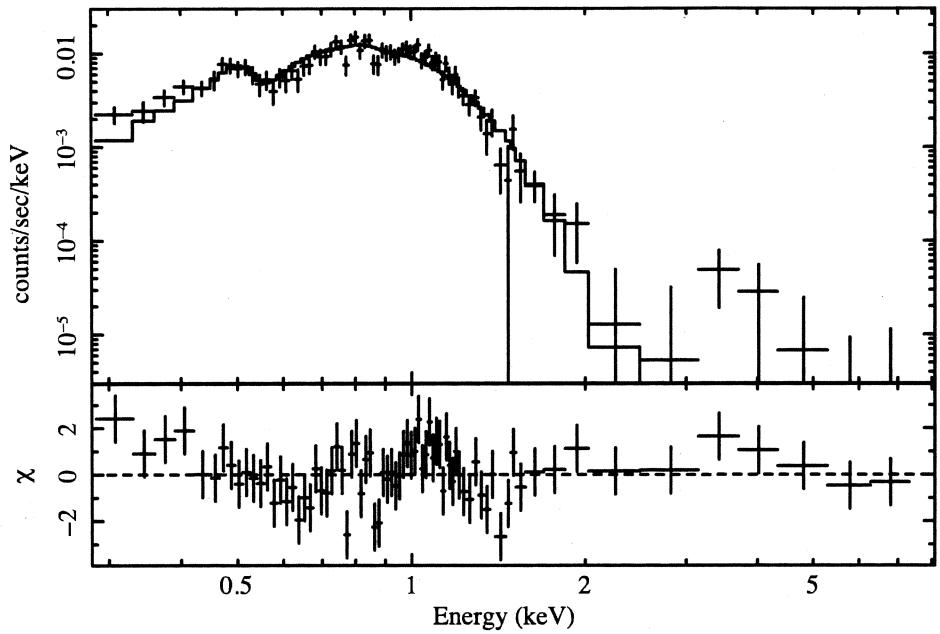

Fig. 3.— *Top panel* : *XMM-Newton* MOS spectrum combined from all the available data. The solid line shows the best-fit model of the spectrum between 0.3−3 keV by an absorbed blackbody model. *Bottom panel* : the residuals of the χ^2 fit.